THE JOURNAL OF BIOLOGICAL CHEMISTRY VOL. 286, NO. 27, pp. 24007–24014, July 8, 2011

Interplay between Flavodiiron Proteins and Photorespiration in *Synechocystis* sp. PCC 6803*[S]

Received for publication, January 20, 2011, and in revised form, May 17, 2011 Published, JBC Papers in Press, May 20, 2011, DOI 10.1074/jbc.M111.223289

Yagut Allahverdiyeva[‡], Maria Ermakova[‡], Marion Eisenhut[‡1], Pengpeng Zhang[‡], Pierre Richaud[§¶‖], Martin Hagemann[**], Laurent Cournac[§¶‖], and Eva-Mari Aro[‡2]

From the [‡]Laboratory of Molecular Plant Biology, Department of Biochemistry and Food Chemistry, University of Turku, FI-20014 Turku, Finland, [§]Commissariat à l'Energie Atomique (CEA), Direction des Sciences du Vivant, Institut de Biologie Environementale et Biotechnologie, Laboratoire de Bioénergétique et Biotechnologie des Bactéries et Microalgues, CEA Cadarache, F-13108 Saint-Paul-lez-Durance, France, [¶]CNRS, UMR Biologie Végétale et Microbiologie Environnementales, F-13108 Saint-Paul-lez-Durance, France, [‖]Aix-Marseille Université, F-13108 Saint-Paul-lez-Durance, France, and the [**]Institut Biowissenschaften, Pflanzenphysiologie, Universität Rostock, Albert-Einstein-strasse 3, D-18059 Rostock, Germany

Flavodiiron (Flv) proteins are involved in detoxification of O_2 and NO in anaerobic bacteria and archaea. Cyanobacterial Flv proteins, on the contrary, function in oxygenic environment and possess an extra NAD(P)H:flavin oxidoreductase module. *Synechocystis* sp. PCC 6803 has four genes (*sll1521*, *sll0219*, *sll0550*, and *sll0217*) encoding Flv proteins (Flv1, Flv2, Flv3, and Flv4). Previous *in vitro* studies with recombinant Flv3 protein from *Synechocystis* provided evidence that it functions as a NAD(P)H: oxygen oxidoreductase, and subsequent *in vivo* studies with *Synechocystis* confirmed the role of Flv1 and Flv3 proteins in the Mehler reaction (photoreduction of O_2 to H_2O). Interestingly, homologous proteins to Flv1 and Flv3 can be found also in green algae, mosses, and *Selaginella*. Here, we addressed the function of Flv1 and Flv3 in *Synechocystis* using the Δ*flv1*, Δ*flv3*, and Δ*flv1*/Δ*flv3* mutants and applying inorganic carbon (C_i)-deprivation conditions. We propose that only the Flv1/Flv3 heterodimer form is functional in the Mehler reaction *in vivo*. $^{18}O_2$ labeling was used to discriminate between O_2 evolution in photosynthetic water splitting and O_2 consumption. In wild type, ~20% of electrons originated from water was targeted to O_2 under air level CO_2 conditions but increased up to 60% in severe limitation of C_i. Gas exchange experiments with Δ*flv1*, Δ*flv3*, and Δ*flv1*/Δ*flv3* mutants demonstrated that a considerable amount of electrons in these mutants is directed to photorespiration under C_i deprivation. This assumption is in line with increased transcript abundance of photorespiratory genes and accumulation of photorespiratory intermediates in the WT and to a higher extent in mutant cells under C_i deprivation.

Flavodiiron proteins (or A-type flavoproteins, Flv)[3] are involved in the detoxification of O_2 or NO in strict and facultative anaerobic prokaryotes (1). A similar type of Flv proteins, however, with strict selectivity toward O_2, was recently identified also in some eukaryotic pathogenic protozoa (2). All of these Flv proteins contain two redox centers: a flavin mononucleotide, functioning as an electron acceptor, and a non-heme Fe-Fe center as an active site (1). Available crystal structures of the Flv proteins from prokaryotic and eukaryotic organisms contain two monomers in a "head-to-tail" arrangement, bringing the flavin mononucleotide and Fe-Fe centers of opposing monomers into close proximity (3, 4).

The genome sequence of the cyanobacterium *Synechocystis* has revealed four genes (*sll1521*, *sll0219*, *sll0550*, and *sll0217*) encoding Flv proteins (Flv1, Flv2, Flv3, and Flv4, respectively). Unlike the organisms mentioned above, cyanobacterial Flv proteins possess an additional NAD(P)H:flavin oxidoreductase module fused at the C terminus (1, 5). Two Flv proteins in *Synechocystis*, Flv2 and Flv4, are unique for cyanobacteria. Interestingly, homologous proteins to Flv1 and Flv3 can be found also in green algae, mosses, and *Selaginella* (6), whereas only one protein with very low similarity to Flv proteins has been found in plant genomes (7). We have recently demonstrated an essential role of Flv2 and Flv4 in photoprotection of the photosystem (PS) II complex under ambient CO_2 conditions (6). Nevertheless, the exact mechanism underlying this photoprotective effect and the localization of the Flv2 and Flv4 proteins still remain to be elucidated.

In vitro studies with recombinant Flv protein from *Synechocystis* provided evidence that Flv3 functions as a NAD(P)H: oxygen oxidoreductase (5), and subsequent *in vivo* studies with *Synechocystis* confirmed the role of Flv1 and Flv3 proteins in photoreduction of O_2 (7). Photoreduction of O_2 to hydrogen peroxide (H_2O_2) at the reducing side of PSI complex was discovered 60 years ago by Mehler in spinach chloroplasts and therefore is called a Mehler reaction (8). Subsequently, it has been reported that the primary product of the Mehler reaction

* This work was supported by Academy of Finland Center of Excellence Project 118637, the European Union Project Solar-H2 (FP7 Contract 212508), CNRS/Japan Science and Technology Agency (Program "Structure and Function of Biomolecules: Response Mechanism to Environments"), and the Nordic Energy Research Program (Project Nordic BioH_2). This work was also supported by the HélioBiotec platform (funded by the European Union (European Regional Development Fund)), the Région Provence Alpes Côte d'Azur, the French Ministry of Research, and the Commissariat à l'Energie Atomique.

[S] The on-line version of this article (available at http://www.jbc.org) contains supplemental Table S1 and Figs. S1–S4.

[1] Present address: Institute of Plant Biochemistry, Heinrich-Heine-Universität, D-40225 Düsseldorf, Germany.

[2] To whom correspondence should be addressed: Laboratory of Molecular Plant Biology, Dept. of Biochemistry and Food Chemistry, University of Turku, FI-20014 Turku, Finland. Fax: 358-23338075; E-mail: evaaro@utu.fi.

[3] The abbreviations used are: Flv, A-type flavodiiron proteins; C_i, inorganic carbon; ROS, reactive oxygen species; RT-q-PCR, real-time quantitative RT-PCR; Chl, chlorophyll; IAC, iodoacetamide; LHCII, light-harvesting complex; PSI, photosystem I; PSII, photosystem II; 2PG, 2-phosphoglycolate; Rubisco, ribulose-1,5-bisphosphate carboxylase/oxygenase.

is superoxide anion (O_2^-), and its disproportionation produces H_2O_2 and O_2 (9). It is important to note that reactive oxygen species (ROS) produced during photoreduction of O_2 do not accumulate in intact chloroplasts due to efficient ROS-scavenging enzymes in near proximity to the photosynthetic electron transport chain (10). Contrary to the Mehler reaction in plants, the cyanobacterial Mehler reaction driven by Flv1 and Flv3 does not produce ROS (7).

In addition to the Mehler reaction and dark respiration, photorespiration consumes O_2 in oxygenic photosynthetic organisms (11) but, in this case, also liberates CO_2. Photorespiration is based on the dual function of Rubisco, the key enzyme of photosynthetic carbon assimilation, which binds either CO_2 or O_2 to the active site depending on the partial pressure of these gases. Oxygenation of ribulose-1,5-bisphosphate by Rubisco produces toxic 2-phosphoglycolate (2PG), which is metabolized by the photorespiratory pathway. Photorespiration is often described as one of the most wasteful reactions due to loss of photosynthetically fixed carbon and energy (12). Cyanobacteria have evolved sophisticated CO_2-concentrating mechanisms that operate to increase the CO_2 concentration around Rubisco, inside of the subcellular compartment called the carboxysome (13–16). The presence of efficient CO_2 concentrating mechanisms suggested that the photorespiratory pathway is probably not essential in cyanobacteria (17). Nevertheless, more recent studies on *Synechocystis* mutants defective in all three predicted photorespiratory pathways, the plant-like C2 cycle and the bacterial-type glycerate and decarboxylation pathways, demonstrated a high CO_2-requiring phenotype comparable with plant photorespiratory mutants and thus supported the existence and essential function of photorespiratory 2PG metabolism in cyanobacteria (18, 19). In addition to 2PG detoxification, the photorespiratory 2PG metabolism together with the Mehler reaction supports the acclimation of cyanobacteria to high light stress because a double mutant Δ*flv3*/Δ*gcvT* defective in both the Flv3 protein and the glycine decarboxylase complex, which is involved in plant-like C2 photorespiratory pathway, could not segregate completely, and the mutant demonstrated a high light-sensitive phenotype (20).

However, despite the well defined routes for 2PG metabolism, the experimental evidence for photorespiratory gas exchange in cyanobacteria is still missing. Here, for the first time to the knowledge of the authors, we report photorespiratory oxygen uptake by Rubisco under C_i deprivation conditions in *Synechocystis* mutant strains deficient in the *flv1* and/or *flv3* genes.

EXPERIMENTAL PROCEDURES

Strain and Culture Conditions—*Synechocystis* sp. PCC 6803 (WT) and mutant strains were grown in BG-11 medium buffered with 20 mM *N*-[Tris(hydroxymethyl)methyl]-2-aminoethanesulfonic acid-KOH, pH 8.2, with gentle agitation under continuous light (50 μmol photons m^{-2} s^{-1}) at 30 °C and 3% CO_2. Three days before the experiments, the cells were shifted to air level CO_2 atmosphere. For measurements, the cells were harvested and resuspended in a fresh BG-11 medium without $NaHCO_3$ at chlorophyll (Chl) concentration of 10–20 μg ml^{-1}. Only when indicated, $NaHCO_3$ was added. For C_i deprivation experiments, the cells were incubated under the light in an airtight Eppendorf tube for 4 h.

Mutants—The construction of the single mutants Δ*flv1* (containing a chloramphenicol-resistant cassette) and Δ*flv3* (containing a spectinomycin-resistant cassette) was described previously (7). The double mutant of Δ*flv1*/Δ*flv3* was generated by second transformation of the Δ*flv3* mutant with the mutated *flv1* construct. The genotype of all mutants was verified by PCR using total chromosomal DNA and gene-specific primers for *flv1* and *flv3* (20), respectively (supplemental Fig. S1).

Oxygen Evolution—Steady-state oxygen evolution rates were measured with a Clark type oxygen electrode (DW1, Hansatech) at a saturating light intensity. To measure the net photosynthesis, the cells were suspended in BG-11 medium supplemented with 10 mM $NaHCO_3$, and for the PSII activity measurements, 2 mM 2,5-dimethyl-*p*-benzoquinone was added to cell suspension as an artificial electron acceptor.

P700 Light Curve Measurements—P700 measurements were performed by DUAL-PAM-100 (Walz, Germany). The yield of non-photochemical energy dissipation in the PSI centers occurring due to the acceptor side limitation of PSI, Y(NA), were calculated as $Y(NA) = (P_m - P_m')/P_m$. For determination of P_m, a saturating pulse (6000 μmol photons m^{-2} s^{-1}, 300 ms) was applied on cell samples preilluminated with far-red light (75 watts m^{-2}, 10 s). Thus, P_m was defined as a maximal change of the P700 signal upon transformation of P700 from the fully reduced to the fully oxidized state. P_m' represents the maximal change of the P700 signal upon application of a saturating pulses at different increasing light intensities duration of 30 s.

Membrane Inlet Mass Spectrometry—Measurements of $^{16}O_2$ (mass 32), $^{18}O_2$ (mass 36) and CO_2 (mass 44) exchange were performed by membrane inlet mass spectrometry directly on culture suspensions. For analyses, 1.5-ml samples were introduced into the measuring chamber that is connected to the vacuum line of a mass spectrometer (model Prima-B, Thermo Fisher Scientific) by a Teflon membrane located at the bottom of the chamber. With this setup, gases dissolved in the liquid above the membrane diffuse through the thin Teflon layer and are directly introduced into the ion source of the mass spectrometer. The measuring chamber was thermostated (30 °C) using a water jacket, and the suspension was continuously mixed by a magnetic stirrer. Actinic light (500 μmol photons m^{-2} s^{-1}) was applied by a LED-powered fiber optic illuminator (PerkinElmer Life Sciences) when needed. Calculation of light-induced oxygen uptake is based on the fact that by photosynthetic activity the cells produce essentially $^{16}O_2$ from water, whereas if the heavy isotope $^{18}O_2$ is present in the suspension, its consumption reflects O_2 uptake. Using a mixture of isotopes, photosynthetic and respiratory activity of cells can then be calculated simultaneously upon illumination using simple isotope ratio expressed either as exchange rates (uptake or production flow rates) or as cumulative O_2 exchange (amounts that have been produced or consumed as a function of time) as detailed in Ref. 21. In our experiments, $^{18}O_2$ (99% $^{18}O_2$ isotope content, Euriso-Top) was injected by bubbling at the top of the suspension just before vessel closure and gas exchange measurements.

Real-time Quantitative RT-PCR (RT-q-PCR)—Total RNA was extracted by TRIsure (Bioline) treatment and purified with

TABLE 1

Photosynthetic activities of *Synechocystis* WT and the mutant cells

The activity of PSII and the net photosynthetic rate were measured as the steady-state oxygen evolution rate in the presence of 2 mM 2,5-dimethyl-*p*-benzoquinone and 10 mM $NaHCO_3$, respectively. Values are given as a mean ± S.D. from three independent experiments. Dark respiration was monitored by membrane inlet mass spectrometry, and values are given as μmol O_2 mg Chl^{-1} h^{-1}.

	PSII activity	Net photosynthetic activity	Dark respiration
	%	%	
WT	100 ± 2.4	100 ± 1.7	10.4 ± 0.6
Δ*flv1*	110 ± 3.2	92 ± 2.1	17.5 ± 1.2
Δ*flv3*	105 ± 1.8	92 ± 1.5	16.1 ± 1.2
Δ*flv1*/Δ*flv3*	95 ± 2.4	89 ± 1.2	13.7 ± 0.7

1 unit of DNase (Ambion Turbo DNase kit) to remove genomic DNA. Purified RNA (1 μg) was used for cDNA synthesis. Reverse transcription was performed with random hexamers (Promega) and SuperScript III Reverse Transcriptase (Invitrogen) according to the manufacturer's protocol. Synthesized cDNA was diluted 5-fold and used as a template for RT-q-PCR.

The RT-q-PCR was performed on a Bio-Rad IQ5 system using iQ SYBR Green Supermix (Bio-Rad) with 40 cycles of amplification. Relative changes in gene expression were calculated as described previously (6) using the constitutively expressed *rnpB* gene as a control. The primers used in this study are summarized in supplemental Table S1.

Quantification of Gly and Ser—Free amino acids were extracted from fresh cyanobacterial cell pellets of 2 ml of culture with 80% ethanol at 65 °C for 3 h. After centrifugation, the supernatants were dried by lyophilization and redissolved in 8 mM Na_2HPO_4, pH 6.8. The content of Gly and Ser were determined by HPLC as described in Ref. 22.

Protein Analysis—A soluble fraction of proteins was isolated as described (6). Protein complexes were separated using 6–13% gradient blue native PAGE followed by immunoblotting with the Flv3 protein-specific antibody.

RESULTS

Phenotype and Photosynthetic Properties of Synechocystis Δ*flv1,* Δ*flv3, and* Δ*flv1*/Δ*flv3 Mutant Cells*—Comparative growth characteristics of the WT and the Δ*flv1*, Δ*flv3*, and Δ*flv1*/Δ*flv3* mutant strains were tested in BG11 medium at ambient air. There was no difference between the WT and the single Δ*flv1* and Δ*flv3* or the double mutant Δ*flv1*/Δ*flv3* strains in their growth characteristics under the conditions described above under "Experimental Procedures" (data not shown).

To compare the electron transfer capacities of the WT, Δ*flv1*, Δ*flv3*, and Δ*flv1*/Δ*flv3* strains, the whole chain photosynthetic electron transfer activity and the PSII activity were monitored. In line with our previous report (6), the Δ*flv1* and Δ*flv3* single mutants demonstrated slightly higher PSII activity in the presence of an artificial electron acceptor, but the net photosynthesis rate was 8% lower as compared with the WT (Table 1). The Δ*flv1*/Δ*flv3* double mutant demonstrated only 89% of the activity from water to $NaHCO_3$ measured for the WT (Table 1). Furthermore, the PSII activity of the Δ*flv1*/Δ*flv3* mutant was slightly lower, 95% of that in the WT (Table 1).

Because Flv1 and Flv3 proteins function in accepting electrons beyond PSI, we next measured the yield of non-photochemical energy dissipation in PSI reaction centers *Y*(NA) under high CO_2 conditions. Fig. 1 demonstrates a typical light response curve for WT with a sharp increase in *Y*(*NA*) at very low light intensities, indicating a high acceptor side limitation of PSI due to an incomplete activation of Calvin-Benson cycle, the main terminal electron acceptor. Activation of CO_2 fixation with time and increasing light intensity is reflected in a decline in *Y*(*NA*). The Δ*flv1* (Fig. 1), Δ*flv3* and Δ*flv1*/Δ*flv3* (data not shown) mutants demonstrated significantly higher *Y*(*NA*) parameter with increasing actinic light intensities compared with the WT.

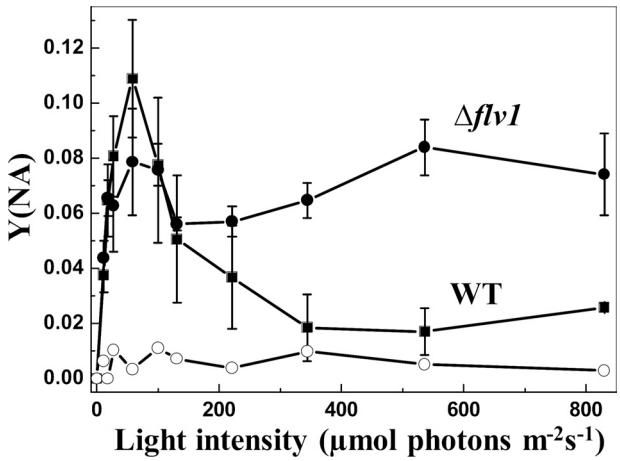

FIGURE 1. **Light response of the acceptor side limitation of PSI, *Y*(NA).** The acceptor side limitation of PSI was recorded from the WT (■) and Δ*flv1* (●) mutant strain. 0.1 mM methyl viologen (○) was added to Δ*flv1* cell suspension before the measurement. Values are the mean ± S.D. from three independent experiments.

The results described above to demonstrate the acceptor side limitation of PSI were verified by using methyl viologen as an artificial acceptor of electrons. Addition of methyl viologen to *Synechocystis* cell suspension before *Y*(*NA*) measurements completely eliminated the acceptor side limitation of PSI in the Δ*flv1* mutant cells (Fig. 1).

Respiration, Photoreduction of O_2 and CO_2 Uptake in Flv Mutants—*Y*(*NA*) measurements demonstrated an important role for the Flv1 and Flv3 proteins in alleviation of the acceptor side electron pressure in PSI. This could be assigned to the function of the Flv1 and Flv3 proteins in donation of electrons to molecular oxygen in the Mehler reaction. This process might be strongly regulated also by other electron transfer routes. To verify this, the WT and the Flv mutants were subjected to detailed gas exchange measurements. The respiratory O_2 uptake was monitored during the dark period, and the photoreduction of O_2 as well as the CO_2 uptake were measured during the dark-light transition by applying the membrane inlet mass spectrometry gas exchange analysis system (21). All Flv mutants, the Δ*flv1* (17.5 μmol O_2 mg Chl^{-1} h^{-1}) and Δ*flv3* (16.1 μmol O_2 mg Chl^{-1} h^{-1}) single mutants as well as the Δ*flv1*/Δ*flv3* (13.7 μmol O_2 mg Chl^{-1} h^{-1}) double mutant demonstrated increased dark respiration rate as compared with the WT (10.4 μmol O_2 mg Chl^{-1} h^{-1}, Table 1). On the other hand, the WT cells and all of the Flv mutants, Δ*flv1*, Δ*flv3*, and Δ*flv1*/Δ*flv3*, showed very similar CO_2 uptake after switching on the actinic light (Fig. 2).

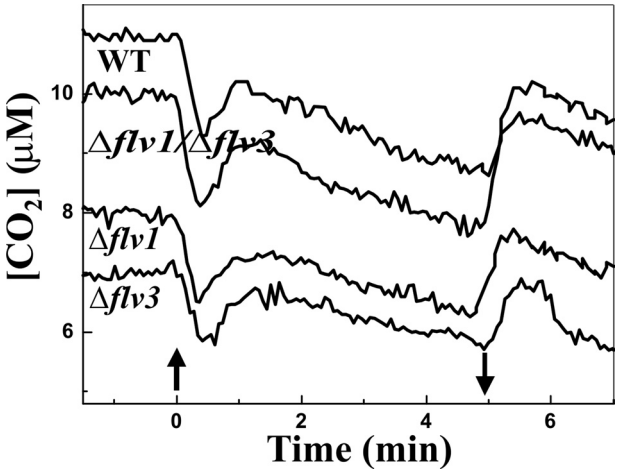

FIGURE 2. **Mass spectrometric measurements of CO_2 uptake during dark-light transition.** During measurement, the cells were first kept in darkness for 5 min, and thereafter the white light of 500 μmol photons m^{-2} s^{-1} was turned on (*upward arrow*) and off again (*downward arrow*).

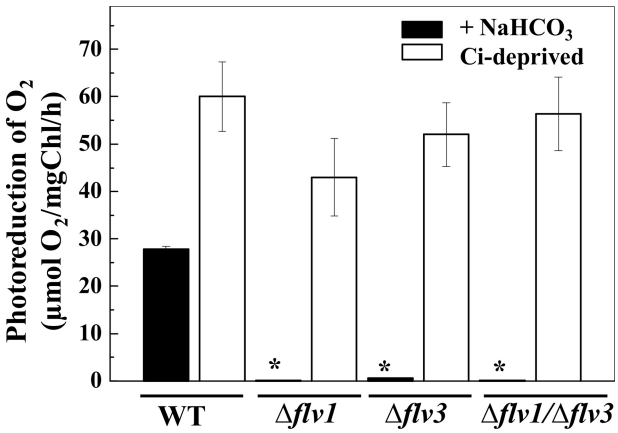

FIGURE 3. **Mass spectrometric measurements of O_2 consumption during dark-light transition in the WT, Δ*flv1*, Δ*flv3*, and Δ*flv1*/Δ*flv3* mutants of *Synechocystis*.** The cells were kept in darkness for 5 min and then illuminated with white light of 500 μmol photons m^{-2} s^{-1} for 5 min to measure the uptake of O_2. The *asterisk* represents cells demonstrated only trace amount of $^{18}O_2$ consumption. *White bars*, 5 mM $NaHCO_3$ was present in the medium. *Black bars*, measurements were performed with the cells exposed to C_i deprivation. Values are the mean ± S.D. from three independent experiments.

$^{18}O_2$ labeling of the cells was then used to separately analyze the evolution and uptake of O_2 during illumination of the cells. In the WT cells, illumination strongly stimulated O_2 uptake (28 μmol O_2 mg Chl^{-1} h^{-1}) in the presence of 5 mM $NaHCO_3$ (Fig. 3). Under the same conditions, the Δ*flv1* and Δ*flv3* single mutant cells did not show any photoreduction of O_2, which is in line with previous studies (Fig. 3) (7). Likewise, the double mutant Δ*flv1*/Δ*flv3* was not able to consume O_2 during illumination in the presence of $NaHCO_3$.

The above experiments confirmed the involvement of both the Flv1 and Flv3 proteins in the Mehler reaction of *Synechocystis*. The next question to be addressed was whether there is a competition between electrons from water oxidation to the Mehler reaction, photorespiration, and CO_2 fixation. To this end, the cell culture was depleted of CO_2, the main terminal electron acceptor of the photosynthetic electron transfer chain. For this purpose, the cells were kept in tightly closed Eppendorf tubes for 4 h. In the absence of dissolved CO_2 and without

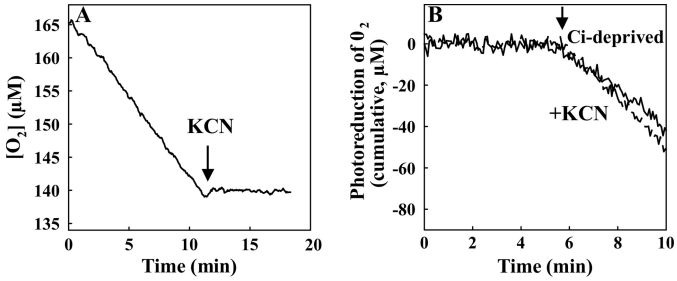

FIGURE 4. **Effect of KCN on dark respiration and photoreduction of O_2.** Dark respiration (*A*) and O_2 photoreduction (*B*) were monitored after addition of KCN (final concentration, 1 mM) (*dashed line* in *B*) to C_i-deprived Δ*flv1*/Δ*flv3* cells. Arrays indicate the addition of inhibitor (*A*) and switching on the actinic light (*B*). In *B*, the cumulative O_2 uptake curve is calculated from $^{18}O_2/^{16}O_2$ exchange measurements and is presented here after subtraction of the dark O_2 uptake rate for better legibility.

exogenously added bicarbonate (C_i deprivation), the WT cells demonstrated enhanced light-induced O_2 uptake compared with that measured in control conditions in the presence of bicarbonate (Fig. 3). Surprisingly, such severe C_i deprivation conditions were found to stimulate the photoreduction of O_2 also in the Δ*flv1* and Δ*flv3* single mutants. These data were first understood to indicate that the Flv1 or Flv3 protein can function in the Mehler reaction as a homodimer under specific conditions such as C_i deprivation. To test this assumption, we generated the double mutant Δ*flv1*/Δ*flv3*. Intriguingly, the Δ*flv1*/Δ*flv3* double mutant also demonstrated a similar O_2 photoreduction rate under C_i deprivation conditions as the single mutants (Fig. 3), thus excluding the possibility of functional Flv1 or Flv3 homodimers. The similar behavior of both the Flv mutants as well as the WT provided evidence that the O_2 photoreduction under C_i deprivation conditions could have an origin different from the Flv1- and Flv3-mediated Mehler reaction.

Because the enhancement of O_2 photoreduction upon C_i deprivation can, in principle, originate from enhanced function of respiratory terminal oxidases, photorespiration, or electron flux from PSI or stromal components directly to O_2 (classical plant-type Mehler reaction), the origin of the O_2 photoreduction was further studied by applying specific inhibitors. The addition of KCN, an inhibitor of terminal oxidases, completely abolished dark respiration (Fig. 4*A*) but did not significantly affect the photoreduction of O_2 in the Δ*flv1*/Δ*flv3* mutant cells (Fig. 4*B*).

Photoreduction of O_2 was next measured in the presence of iodoacetamide (IAC), a widely used inhibitor of CO_2 fixation and photorespiration (7, 23). Measurements with cell suspensions supplemented with IAC were first performed in the presence of bicarbonate. In such conditions, the addition of IAC strongly stimulated the rate of O_2 photoreduction in WT (Fig. 5*A*), whereas in the Δ*flv1* (supplemental Fig. S2*A*) and Δ*flv3* (supplemental Fig. S2*B*) single mutants as well as in the Δ*flv1*/Δ*flv3* double mutant (Fig. 5*B*) the stimulation of O_2 photoreduction was only modest.

We next proceeded to compare the effect of IAC on photoreduction of O_2 at C_i deprivation conditions. As demonstrated previously in Fig. 3, the WT as well as all the Flv mutant cells showed strong O_2 photoreduction at C_i deprivation (Fig. 5, *C*

and *D*, for WT and Δ*flv1*/Δ*flv3*, respectively). It is conceivable that the C_i deprivation favors the oxygenation of RuBP and thus photorespiratory 2PG metabolism. The addition of IAC to the C_i-deprived WT cell suspension to inhibit the CO_2 fixation and photorespiration did not significantly change O_2 photoreduction (Fig. 5*C*). In sharp contrast to the WT, addition of IAC to the Δ*flv1*, Δ*flv3* (supplemental Fig. S2, *C* and *D*, respectively), and Δ*flv1*/Δ*flv3* double mutant cells abolished ~75% of O_2 photoreduction (Fig. 5*D*). High sensitivity of O_2 photoreduction to IAC, the Calvin-Benson cycle inhibitor, during C_i deprivation, led us to conclude that the C_i-sensitive O_2 photoreduction in the Δ*flv1* and Δ*flv3* mutants as well as in the Δ*flv1*/Δ*flv3* double mutant is mainly due to photorespiration, *i.e.* oxygenase function of Rubisco. Similar results were obtained when cell suspension was supplemented with glycolaldehyde (supplemental Fig. S4), another effective inhibitor of the photosynthetic carbon reduction cycle (24). About 25% of O_2 photoreduction in the Δ*flv1*, Δ*flv3*, and Δ*flv1*/Δ*flv3* mutant cells was insensitive to IAC (Fig. 5*D*), and this might originate from the electron flux from the PSI complex directly to O_2 or from a fraction of Rubisco that was not fully inhibited by the inhibitor. It was also tested that IAC has no effect on the function of terminal oxidases in the dark (Fig. S3).

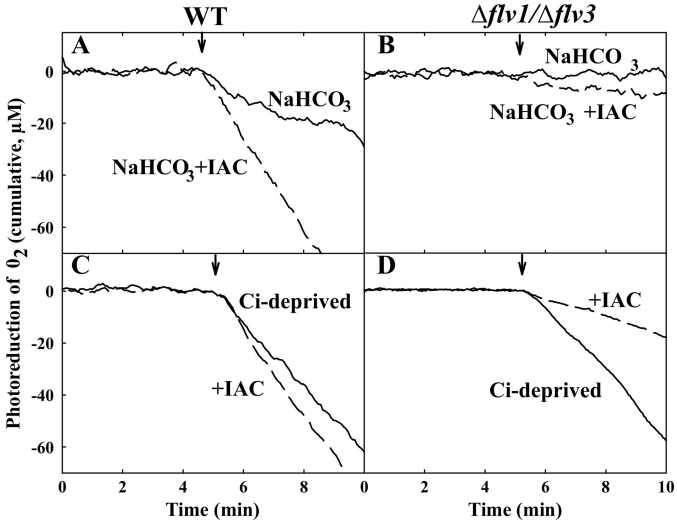

FIGURE 5. **Effect of IAC on photoreduction of O_2 in the WT and Δ*flv1*/Δ*flv3* cells.** O_2 photoreduction was monitored in the presence of 5 mM $NaHCO_3$ (*solid line*) and in the presence of both 5 mM $NaHCO_3$ and 8 mM IAC (*dashed line*) from the WT (*A*) and Δ*flv1*/Δ*flv3* mutant cells (*B*). Similar measurements were performed from the WT (*C*) and Δ*flv1*/Δ*flv3* (*D*) cells after C_i deprivation. Arrays indicate switching on the light. Cumulative O_2 uptake curve was calculated from $^{18}O_2/^{16}O_2$ exchange measurements and is presented here after subtraction of dark O_2 uptake rate for better legibility.

Photorespiratory Pathway—To support the assumption of an activated photorespiratory 2PG cycle in C_i-limited WT and Flv mutant cells, the relative expression level of two genes, *gcvT* (*sll0171*) and *ilvB* (*sll1981*), encoding the Gly decarboxylase complex T protein and glyoxylate carboligase, involved in the plant-like C2 cycle and bacterial-type glycerate photorespiratory pathways, respectively, were analyzed by RT-q-PCR. The relative transcript abundance of these genes was studied in the WT and Δ*flv1*/Δ*flv3* mutant cells from three different conditions: (i) high CO_2 grown cells where the occurrence of photorespiratory pathway is minimal, (ii) after C_i deprivation treatment where enhanced photorespiratory metabolism is expected, and (iii) after addition of IAC to C_i-deprived cells. Under C_i deprivation conditions, the transcript levels of the *gcvT* and *ilvB* genes were ~2–3-fold higher in both the WT and Δ*flv1*/Δ*flv3* mutant cells as compared with high CO_2 grown cells (Fig. 6*A*). On the contrary, addition of IAC significantly decreased the transcript level of both genes. It is important to note that even in high CO_2 grown cells, the transcripts of *gcvT* and especially of *ilvB* genes were much more abundant in the Δ*flv1*/Δ*flv3* mutant cells as compared with the WT.

Gly and Ser, the photorespiratory intermediates, were also monitored in the WT and mutant cells. After 12 h of incubation under C_i deprivation conditions, all cells showed a clear accumulation of Gly and Ser, indicating an enhanced flux into the plant-like C2 photorespiratory cycle. Although WT cells acclimate after longer times, resulting in a decrease in Gly content, the Δ*flv1* and Δ*flv3* mutant cells still demonstrated a high accumulation of both amino acids (Fig. 6*B*). Obviously, severe C_i deprivation does lead to the accumulation of intermediates of the plant-like 2PG pathway despite the slight increase in transcript level of some photorespiratory genes during the active photorespiration.

Dimerization of Flv Proteins—Because the Flv proteins from different organisms have demonstrated a homodimer or homotetramer organization *in vitro* (3–5), we addressed the question about dimerization of *Synechocystis* Flv proteins. Both Flv1 and

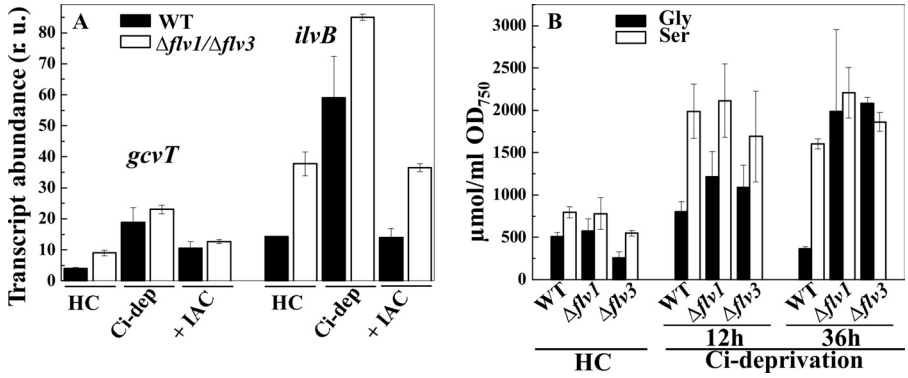

FIGURE 6. **Effect of C_i deprivation on photorespiratory markers.** *A*, transcript abundance of the *gcvT* and *ilvB* genes in the WT (*black bars*) and Δ*flv1*/Δ*flv3* (*white bars*) cells. Samples were taken from the cells grown in the presence of 3% CO_2 (*HC*), after 12 h shift from HC to C_i deprivation conditions (*C_i-dep*) and after 4 h treatment with IAC of the samples incubated at C_i deprivation for 8 h (+IAC). *r.u.*, relative units. *B*, accumulation of Gly and Ser in the WT, Δ*flv1*, and Δ*flv3* cells. Samples were taken from the cells grown in the presence of 3% CO_2, after a 12- and 36-h shift from HC to C_i deprivation conditions.

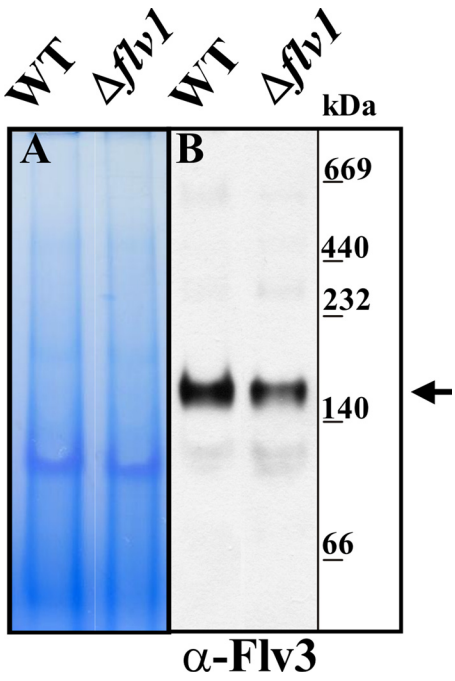

FIGURE 7. **Dimerization of the Flv1 and Flv3 proteins in the WT and mutant cells.** Soluble fraction of cellular proteins was isolated as described (6). Protein complexes were separated using 6–13% gradient blue native PAGE electrophoresis (*A*) and immunodetected with Flv3 antibody (*B*). The *arrow* indicates the location of the Flv3 protein where it is present as a dimer with molecular mass of ~140 kDa. The molecular mass of the Flv monomer is 70 kDa. Gels were loaded on a protein basis.

Flv3 are soluble proteins in the cytoplasm (6). To determine whether the Flv1 and Flv3 proteins are dimerized *in vivo*, the soluble protein fraction was isolated from the WT and Δ*flv1* mutant cells, subjected to blue native PAGE, and immunoblotted with the Flv3 antibody. As shown in Fig. 7*B*, the Flv3 antibody in the WT cells recognized a major band above the 140-kDa marker, suggesting that most of the Flv3 proteins are present as a homo- or heterodimer. However, the Flv1 antibody did not recognize the protein in *Synechocystis* cell extracts but only when overexpressed in *Synechocystis* or *Escherichia coli*, thus being in accordance with a very low transcript level of the *flv1* gene in the cells (6). Accordingly, this antibody could not be used to analyze the 140-kDa band. The presence of a protein band with similar molecular mass also in the Δ*flv1* mutant cells indicated that the Flv3 protein is capable of forming homodimers as well. However, the similar behavior of the Δ*flv1*/Δ*flv3* double mutant and both of the Flv single mutants in the photoreduction of O_2 in the presence of bicarbonate and in C_i deprivation, suggested that the Flv3 or Flv1 homodimers are not active in the Mehler reaction *in vivo*. In line with functional significance of the heterodimer, the accumulation of the Flv3 protein was dependent on the presence of the Flv1 protein, as the amount of the Flv3 protein was significantly down-regulated in the Δ*flv1* mutant cells (Fig *7B*).

DISCUSSION

Mehler Reaction Is a Strong Sink of Electrons in Cyanobacteria—In plant chloroplasts, the Mehler reaction plays a protective role acting as a sink for excess electrons under severe stress conditions, for example when CO_2 fixation is impaired (25). This reaction leads to the production of ROS. As a consequence, plants have during the evolution developed a strong ROS-scavenging system (26). It is intriguing to note that cyanobacteria, the progenitors of chloroplasts, employ a completely different strategy for performing Mehler reactions. The Flv1 and Flv3 proteins, performing the Mehler reaction in cyanobacteria (Fig. 3), can reduce O_2 to water without generation any ROS. It has been proposed that the Mehler reaction in cyanobacteria is evolutionarily related to the response of anaerobic bacteria to O_2 (7).

Assuming that the O_2 photoreduction in the WT *Synechocystis* cells in the presence of saturated amount of C_i is mainly due to the Mehler reaction operated via Flv1 and Flv3, the cells pass ~20% of electrons originating from PSI to O_2 via the Flv1/Flv3 heterodimer. At C_i deprivation conditions, the O_2 photoreduction rate was 50–60% of gross photosynthetic O_2 evolution in the WT *Synechocystis* cells. Because IAC, the inhibitor of CO_2 fixation and photorespiration, was found to have a stimulatory effect on photoreduction of O_2, to a larger extent in the presence of C_i than in C_i deprivation, the capacity of the Mehler reaction is likely to be very high. This is deduced from the fact that IAC, by inhibiting the CO_2 uptake in the presence of C_i and suppressing possible electron flux via photorespiration under the C_i deprivation, stimulates Mehler reaction to a larger extent in the WT. Thus, the Mehler reaction seems to function as an efficient sink of electrons and thereby dissipates excess energy in the photosynthetic apparatus of *Synechocystis*. Nevertheless, it is likely that cyanobacteria with efficient CO_2 concentrating mechanism only seldom use their Mehler reaction in its full capacity.

Even though dimerization is a general feature of *Synechocystis* Flv proteins, only the Flv1/Flv3 heterodimer was found to be a physiologically functional form in the Mehler reaction *in vivo*. A significant decrease in the amount of Flv3 in the Δ*flv1* mutant also suggests that the stability of the Flv1 and Flv3 proteins is co-regulated. We do not, however, exclude the possibility that homodimers of Flv1 and Flv3 might be formed at least in the mutant background that could have another, still unknown function in cells.

Evidence for Functional Photorespiratory Gas Exchange in Cyanobacteria—In addition to the Mehler reaction in WT cells, it was intriguing to note that the Flv mutants are also capable to direct 40–60% of electrons from the photosynthetic electron transfer chain to photoreduction of O_2. At first glance, these results are striking and even contradictory. It should be noted, however, that such strong photoreduction of O_2 was recorded only at severe limitation of C_i under conditions where the WT efficiently directs electrons mainly to the Mehler reaction. Indeed, there is compelling evidence that the mutant strains with inactivated *flv1* and/or *flv3* gene do not perform light-induced O_2 uptake when C_i is present as a terminal electron acceptor (Fig. 3) (7). Therefore, significant O_2 photoreduction under severe C_i deprivation in both the Δ*flv1* and Δ*flv3* mutant cells as well as in the double mutant must have a different origin.

In all cyanobacteria, two partially overlapping photorespiratory pathways, one similar to plant photorespiratory metabolism and the other similar to bacterial glycerate pathway, have

been predicted from *in silico* analyses (19). A third metabolic route, the decarboxylation pathway, was suggested recently by Eisenhut *et al.* (18). It was hypothesized that the photorespiratory 2PG metabolism is important for distribution of the crucial intermediate glyoxylate for the synthesis of metabolic precursors and biomass. Recent computational simulations of the *Synechocystis* primary metabolism demonstrated that the majority of Gly and Ser originate from photorespiratory 2PG metabolism at photoautotrophic growth. Only under dark conditions, the much lower glyoxylate demand may be alternatively fulfilled by proline catabolism (27).

Cyanobacteria are evolutionarily the first prokaryotes performing water oxidation, which resulted in high intracellular O_2 level. A strong focus during evolution of oxygenic photosynthetic organisms has been on preventing the damages of self-generated oxidative environment. Additionally, in nature cyanobacteria are often exposed to C_i limitation (28) conditions (for instance, acidic water, low mixing, cyanobacterial mats, etc.), and this would favor the cells to perform photorespiration at higher rates. It is conceivable that the efficient function of the Flv1 and Flv3 proteins in the Mehler reaction in cyanobacteria reduces but does not eliminate the importance of photorespiration in dissipation of excess energy under low C_i conditions. The application of $^{18}O_2$ labeling and the C_i deprivation conditions to the mutant cells without Mehler background clearly demonstrated that the Flv-based Mehler reaction is not the only sink for electrons in C_i deprivation. Indeed, a considerable amount of electrons under such conditions are directed to photorespiratory 2PG metabolism in the Δ*flv1*, Δ*flv3*, and Δ*flv1*/Δ*flv3* mutants. Moreover, our results do not exclude but rather also support a possibility that in WT *Synechocystis* cells, a certain amount of electrons is directed to the detoxification of the oxygenation product 2PG of Rubisco under specific conditions, such as C_i deprivation. In line with our present results, an interaction of the Flv3 protein with photorespiration was suggested to be crucial based on the high light-sensitive phenotype of the double mutant Δ*flv3*/Δ*gcvT* (20).

Evolutionary Implications on Elimination of Cyanobacterial-type and Development of Plant-type Mehler Reaction—Genes encoding the Flv1 and Flv3 type proteins have been found in sequenced genomes of all cyanobacteria as well as in green algae and mosses (6). During evolution of higher plants, the Flv-based Mehler reaction, with water as a direct end product, was lost and became replaced with the plant-type, classical Mehler reaction, which produces ROS, and evolved in concert with an efficient ROS-scavenging system. The plant-type Mehler is unlikely to support significant electron flow, with the estimated values being less than 10% (11), and its function is clearly limited as an electron sink under severe stress conditions. In eukaryotic photosynthetic organisms, the excess energy dissipation and adjustment of the NADPH/ATP ratio is in close communication with mitochondria, which might in some cases divert excess reducing power into (distant) O_2 consumption (29). It is also likely that the elimination of Flv proteins in higher plant chloroplasts was closely related to the movement of life from water to the land. Life in the atmosphere affords intensive gas diffusion, thus avoiding overaccumulation of O_2 in photosynthetic cells and probably making the Flv proteins dispensable. It is conceivable that in higher plants, the regulation of the redox poise in chloroplasts by cyclic electron flow around PSI together with efficient non-photochemical quenching and light-harvesting complex II phosphorylation is enough to provide sufficient photoprotection (30). In aquatic or humid environments, gas diffusion is slower; therefore, a direct scavenging of O_2 via the Flv proteins and without formation of ROS is probably more important for efficient carboxylation of Rubisco. Green algae and mosses represent evolutionary intermediates. Their dissipation of excess energy, for instance by the non-photochemical quenching system, resembles that of higher plants (31–33), but they still harbor the genes involved in the Flv-type Mehler reaction (6). Photorespiratory pathway also functions as an efficient electron sink for dissipation of excess energy in C3 plants, particularly under limiting CO_2 conditions, and accordingly plays a crucial role also in high light acclimation of C3 plants (34, 35). In cyanobacteria, on the contrary, the concerted function of the Flv proteins has the most decisive role in dissipation of excess energy in C_i deprivation and apparently also during dark-light transitions.

Acknowledgments—We thank Dr. N. Battchikova for fruitful discussions and K. Michl for amino acid analyses. Professors A. Kaplan and T. Ogawa are thanked for kindly providing us with the Flv1 and Flv3 knock-out mutants.

REFERENCES

1. Vicente, J. B., Justino, M. C., Gonçalves, V. L., Saraiva, L. M., and Teixeira, M. (2008) *Methods Enzymol.* **437,** 21–45
2. Vicente, J. B., Testa, F., Mastronicola, D., Forte, E., Sarti, P., Teixeira, M., and Giuffrè, A. (2009) *Arch. Biochem. Biophys.* **488,** 9–13
3. Di Matteo, A., Scandurra, F. M., Testa, F., Forte, E., Sarti, P., Brunori, M., and Giuffrè, A. (2008) *J. Biol. Chem.* **283,** 4061–4068
4. Frazão, C., Silva, G., Gomes, C. M., Matias, P., Coelho, R., Sieker, L., Macedo, S., Liu, M. Y., Oliveira, S., Teixeira, M., Xavier, A. V., Rodrigues-Pousada, C., Carrondo, M. A., and Le Gall, J. (2000) *Nat. Struct. Biol.* **7,** 1041–1045
5. Vicente, J. B., Gomes, C. M., Wasserfallen, A., and Teixeira, M. (2002) *Biochem. Biophys. Res. Commun.* **294,** 82–87
6. Zhang, P., Allahverdiyeva, Y., Eisenhut, M., and Aro, E. M. (2009) *PLoS One* **4,** e5331
7. Helman, Y., Tchernov, D., Reinhold, L., Shibata, M., Ogawa, T., Schwarz, R., Ohad, I., and Kaplan, A. (2003) *Curr. Biol.* **13,** 230–235
8. Mehler, A. H. (1951) *Arch. Biochem. Biophys.* **33,** 65–77
9. Asada, K., Kiso, K., and Yoshikawa, K. (1974) *J. Biol. Chem.* **249,** 2175–2181
10. Asada, K. (2006) *Plant Physiol.* **141,** 391–396
11. Badger, M. R., von Caemmerer, S., Ruuska, S., and Nakano, H. (2000) *Philos Trans. R. Soc. Lond B. Biol. Sci.* **355,** 1433–1446
12. Artus, N. N., Somerville, S. C., Somerville, C. R., and Lorimer, G. H. (1986) *CRC Crit. Rev. Plant Sci.* **4,** 121–147
13. Badger, M. R., and Price, G. D. (2003) *J. Exp. Bot.* **54,** 609–622
14. Kaplan, A., and Reinhold, L. (1999) *Annu. Rev. Plant Physiol. Plant Mol. Biol.* **50,** 539–570
15. Price, G. D., Badger, M. R., Woodger, F. J., and Long, B. M. (2008) *J. Exp. Bot.* **59,** 1441–1461
16. Battchikova, N., Eisenhut, M., and Aro, E. M. (2010) *Biochim. Biophys. Acta*, in press
17. Colman, B. (1989) *Aquat Bot.* **34,** 211–231
18. Eisenhut, M., Ruth, W., Haimovich, M., Bauwe, H., Kaplan, A., and Hagemann, M. (2008) *Proc. Natl. Acad. Sci. U.S.A.* **105,** 17199–17204
19. Bauwe, H., Hagemann, M., and Fernie, A. R. (2010) *Trends Plant Sci.* **15,** 330–336

20. Hackenberg, C., Engelhardt, A., Matthijs, H. C., Wittink, F., Bauwe, H., Kaplan, A., and Hagemann, M. (2009) *Planta* **230,** 625–637
21. Dimon, B., Gans, P., and Peltier, G. (1988) *Methods Enzymol.* **167,** 686–691
22. Hagemann, M., Vinnemeier, J., Oberpichler, I., Boldt, R., and Bauwe, H. (2005) *Plant Biol.* **7,** 15–22
23. Wildner, G. F., and Henkel, J. (1976) *Biochem. Biophys. Res. Commun.* **69,** 268–275
24. Miller, A. G., and Canvin, D. T. (1989) *Plant Physiol.* **91,** 1044–1049
25. Johnson, X., Wostrikoff, K., Finazzi, G., Kuras, R., Schwarz, C., Bujaldon, S., Nickelsen, J., Stern, D. B., Wollman, F. A., and Vallon, O. (2010) *Plant Cell* **22,** 234–248
26. Foyer, C. H., and Noctor, G. (2000) *New Phytol.* **146,** 359–388
27. Knoop, H., Zilliges, Y., Lockau, W., and Steuer, R. (2010) *Plant Physiol.* **154,** 410–422
28. Talling, J. F. (1985) in *Inorganic Carbon Uptake by Aquatic Photosynthetic Organisms* (Berry, W. J., ed) American Society of Plant Physiologists, pp. 403–420, Rockville, MD
29. Noguchi, K., and Yoshida, K. (2008) *Mitochondrion* **8,** 87–99
30. Tikkanen, M., Grieco, M., and Aro, E. M. (2011) *Trends Plant Sci.* **16,** 126–131
31. Bonente, G., Passarini, F., Cazzaniga, S., Mancone, C., Buia, M. C., Tripodi, M., Bassi, R., and Caffarri, S. (2008) *Photochem. Photobiol.* **84,** 1359–1370
32. Alboresi, A., Gerotto, C., Giacometti, G. M., Bassi, R., and Morosinotto, T. (2010) *Proc. Natl. Acad. Sci. U.S.A.* **107,** 11128–11133
33. Peers, G., Truong, T. B., Ostendorf, E., Busch, A., Elrad, D., Grossman, A. R., Hippler, M., and Niyogi, K. K. (2009) *Nature* **462,** 518–521
34. Osmond, C. B. (1981) *Biochim. Biophys. Acta* **639,** 77–98
35. Kozaki, A., and Takeba, G. (1996) *Nature* **384,** 557–560